

# PRODUCTION OF ETA-MESONS IN COLLISIONS OF NUCLEONS AND DELTA-RESONANCES <sup>1</sup>

W. PETERS, U. MOSEL, A. ENGEL

*Institut für Theoretische Physik, Universität Giessen*

*D-35392 Giessen, Germany*

## Abstract

We calculate the cross section for the production of  $\eta$ -mesons via  $\Delta N \rightarrow NN\eta$  in a relativistic One-Boson-Exchange-Model. Using this cross section we then determine the probability for the production of an  $\eta$ -meson by a  $\Delta$ -resonance moving in nuclear matter. The result is compared to prescriptions in BUU-calculations in which  $\eta$ -production proceeds both through a direct channel and through the sequential process  $\Delta \rightarrow N\pi; \pi N \rightarrow N\eta$ .

---

<sup>1</sup> *Work supported by BMFT and GSI Darmstadt*

# 1 Introduction

The detection of mesons produced in heavy-ion-collisions is an important means for the investigation of the behavior of nuclear matter under extreme conditions. An analysis of pion spectra, for example, has shown that within the reaction zone, where at bombarding energies of about 1 GeV per nucleon baryon densities up to  $3\rho_0$  are reached, about a third of the nucleons is excited to  $\Delta$ -resonances [1]. Numerical simulations of heavy-ion-collisions arrive at the same result [2].

A direct consequence of this resonance matter formation is in these calculations an enhancement of sub-threshold particle production [3, 4]. If the bombarding energy per nucleon is below the free threshold for the production of a particle, even when Fermi motion is taken into account, then a large part of the observed reaction cross section is, according to numerical simulations, due to entrance channels involving resonances; these resonances store energy which can then be used to produce this particle.

While the calculated particle yields generally agree quite well with experiment when the resonance channels are included, it is clear that this result depends on the cross sections used for the production processes involving resonances in the entrance channel; the BUU-calculations mentioned just use an ad-hoc recipe for the direct reaction channel  $\Delta N \longrightarrow NN\text{meson}$  and contain an explicit treatment of the sequential channel  $\Delta \rightarrow N\pi; \pi N \rightarrow N\eta$ .

It is thus the aim of this study to investigate the elementary production process in more detail in order to put the results on the dominance of resonance channels on a firmer ground. For this study we chose the process  $\Delta N \rightarrow NN\eta$  because all the interaction vertices occurring there are known

from other processes.

## 2 The process $\Delta N \rightarrow NN\eta$

We use a relativistic One-Boson-Exchange-Model to calculate the cross section of the process  $\Delta N \rightarrow NN\eta$ . Models like this have been used successfully to describe the production of  $\eta$ -mesons in collisions between nucleons [5-7].

### 2.1 Couplings

We use the standard interaction-terms in the hadronic Lagrangian. Because the  $\Delta$  has isospin 3/2, the only exchange bosons that have to be taken into account are the isovector mesons  $\pi$  and  $\rho$ .

The interaction-terms involving the pion are (the subscript  $N^*$  always refers to the  $N(1535)$ -resonance):

$$\begin{aligned}\mathcal{L}_{\Delta N \pi} &= \frac{g_{\Delta N \pi}}{m_\pi} \bar{\Psi}_\Delta^\mu \hat{T} \Psi_N \partial_\mu \vec{\pi} + h.c. \\ \mathcal{L}_{NN^* \pi} &= g_{NN^* \pi} \bar{\Psi}_{N^*} \frac{\vec{\tau}}{2} \Psi_N \vec{\pi} + h.c. \quad .\end{aligned}\tag{1}$$

For the interactions containing the  $\rho$ -meson we use:

$$\begin{aligned}\mathcal{L}_{\Delta N \rho} &= i \frac{g_{\Delta N \rho}}{m_\Delta + m_N} \bar{\Psi}_\Delta^\mu \hat{T} \gamma^\nu \gamma_5 \Psi_N (\partial_\mu \vec{\rho}_\nu - \partial_\nu \vec{\rho}_\mu) + h.c. \\ \mathcal{L}_{NN^* \rho} &= i g_{NN^* \rho} \bar{\Psi}_{N^*} \gamma_5 \gamma_\mu \frac{\vec{\tau}}{2} \Psi_N \vec{\rho}^\mu + h.c. \quad .\end{aligned}\tag{2}$$

Finally the coupling of the  $\eta$  is taken to be:

$$\mathcal{L}_{NN^* \eta} = g_{NN^* \eta} \bar{\Psi}_{N^*} \Psi_N \eta + h.c. \quad .\tag{3}$$

The diagrams that are to be considered are shown in Fig. 1 (Top). We neglect pre-emission graphs since these are suppressed kinematically. Graphs, where the  $\eta$  is not produced via a  $N(1535)$  but via a nucleon, are neglected as well, because the  $NN\eta$ -vertex is assumed to be negligible due to an analysis of Bhalearo and Liu [8]. In principle, there could also be a  $N(1535)$ - $\Delta$ - $\pi$ -coupling. However, according to [9] the branching ratio for the decay  $N(1535) \rightarrow \Delta\pi$  is smaller than 1%. Therefore this coupling is clearly negligible.

For the off-shell particles in the diagrams in Fig. 1 (Top). we use monopole form factors:

$$f(q^2) = \frac{\Lambda^2 - m^2}{\Lambda^2 - q^2} \quad (4)$$

## 2.2 Parameters

The value of the  $\Delta$ -nucleon-pion coupling is easily determined using the decay-width of the  $\Delta$ :

$$g_{\Delta N\pi} = 2.15 \quad (5)$$

which corresponds to a  $\Delta$ -width of 115 MeV. This number is rather fixed because of the well known width of the  $\Delta$ .

The experimental values of the  $N(1535)$ -width and its branching ratios have big uncertainties [9]; in order to fix  $g_{NN^*\pi}$  and  $g_{NN^*\eta}$  we therefore consider the process  $\pi N \rightarrow N\eta$ . These coupling-constants were already determined by other groups (for example [5, 8]). However, different models or different energy ranges were employed in these analyses so that we are forced, in order to ensure consistency within the model used, to fix these numbers using our parameterization.

To calculate the cross section for  $\pi N \rightarrow N\eta$  one has to evaluate the diagrams shown in Fig. 1 (Bottom). The couplings  $g_{NN^*\eta}$  and  $g_{NN^*\pi}$  enter in two different ways into these diagrams: First, they appear as factors at the vertices and, second, they enter through the  $N(1535)$ -width in the propagator. The dependence of the  $N(1535)$ -width and its branchingratio on these couplings was determined by evaluating the diagrams for the decay into a pion and an  $\eta$ , respectively. The two-pion decay of the  $N(1535)$  was assumed to give a 10 % contribution to the total width.

Evaluating the diagrams in Fig. 1 (Bottom) numerically and comparing these calculations with the data available for  $\pi N \rightarrow N\eta$  we arrived at the numbers (Fig. 2):

$$\begin{aligned} g_{NN^*\pi} &= 1.37 \\ g_{NN^*\eta} &= 1.53 \end{aligned} \tag{6}$$

The couplings involving the  $\rho$ -meson are harder to determine. However, the following calculations show, that the contribution of the  $\rho$ -exchange is much less important than the exchange of a pion. We, therefore, took the numbers of other groups (e.g. [5]) for these couplings:

$$\begin{aligned} g_{\Delta N\rho} &= 13.3 \\ g_{NN^*\rho} &= 0.61 \end{aligned} \tag{7}$$

(see Sec. 2.4).

### 2.3 Kinematics, the exchanged pion

The kinematics of the reaction  $\Delta N \rightarrow NN\eta$  need further attention, because the exchanged pion can be on-shell. This can be seen from the diagrams

in Fig. 1 (Top): If the exchanged meson is a pion and one simply cuts the meson line, one ends up with two diagrams that are both possible as reactions between on-shell particles. The first one stands for the  $\Delta$ -decay and the second one for the process  $\pi N \rightarrow N\eta$ . A detailed analysis shows, that the pion can be on-shell for cm-energies of the  $\Delta N$ -system from about 50 MeV above the threshold for  $\eta$ -production up to about 7 GeV. In this case the pion propagator becomes infinite, and the integration over the phase space of the final particles cannot be performed because the integral diverges.

The solution to this problem is to remember that the reaction considered here does not take place in the vacuum, but during a heavy-ion-collision, i. e. within a medium with a non-vanishing baryon density. In such a medium the pion acquires an in-medium width which renders the pion propagator finite, so that the total cross section can be calculated.

This width enters into the propagator via the pion selfenergy  $\Sigma_\pi$ :

$$G_\pi = \frac{i}{q^2 - m_\pi^2 - \Sigma_\pi} \quad . \quad (8)$$

The relation between the width and the imaginary part of the pion selfenergy is:

$$\text{Im } \Sigma_\pi = -E_\pi \Gamma_\pi \quad . \quad (9)$$

The width of the pion is nothing else but its inverse lifetime and can therefore be expressed by means of the mean free path:

$$\Gamma_\pi = \frac{1}{\tau} = \frac{v_\pi}{l} = v_\pi \rho \sigma_{\pi N} + \tilde{\Gamma}_\pi(\rho) \quad , \quad (10)$$

where  $v_\pi$  is the pion velocity,  $\rho$  is the nuclear density and  $\sigma_{\pi N}$  is the total pion-nucleon cross section, which contains elastic scattering as well as

inelastic processes [10]. By using the form (10) we assume a local-density approximation for the selfenergy of the pion; we are aware of the fact, that this is a good approximation only in the nuclear bulk matter region.

$\tilde{\Gamma}_\pi(\rho)$  in Eq. (10) represents the part of the selfenergy of the pion which is due to many-body effects in the nuclear medium. The effect of 2- and 3-body absorption on the pion selfenergy in the region of the  $\Delta$ -resonance has been discussed extensively in the literature (e.g. [12, 15]). In the present case however the pion-nucleon system has an invariant mass above the  $\eta$ -threshold where several resonances contribute (N(1440), N(1520), N(1535),...), so that there is no quantitative information available. In the absence of any reliable information on the many-body part of the pion selfenergy we have therefore simply multiplied the  $\pi N$  cross section with a density dependent factor by making the replacement

$$\sigma_{\pi N} \longrightarrow \sigma_{\pi N}(1 + \alpha(\rho)) . \quad (11)$$

with  $\alpha(\rho = 0) = 0$ . Since we will work at constant density (local density approximation), effectively this just amounts to multiplying the cross section  $\sigma_{\pi N}$  with a constant factor.

The expression for the imaginary part of the selfenergy in Eq. (9) can be derived by evaluating the lowest order diagrams contributing to  $\Sigma_\pi$  by means of Cutkosky's rule. For  $\alpha = 0$  it reduces to the well known form  $\text{Im } \Sigma_\pi = -m_\pi \Gamma_\pi$  if one chooses the rest frame of the pion as the reference frame. In our case the more general form (9) must be used, because the width given by (10) uses the rest frame of the medium as the reference frame.

For the real part of the selfenergy we took results of calculations em-

ploying the  $\Delta$ -hole-model [11]. The  $\Delta$ -hole-model also yields an imaginary part of  $\Sigma$  which is similar to (10) [12]. However,  $\sigma_{\pi N}$  then only contains the  $\Delta$  and no other resonances. We improved this by using a parameterization of the experimental data for  $\sigma_{\pi N}$  in (10), thereby including also higher resonances.

An important consequence of Eq. (10) is that because of the density dependence of the pion-width the cross section for  $\Delta N \rightarrow NN\eta$  depends on the density as well. This will be discussed further in the next section.

## 2.4 Results

The results of our calculations for the total cross section are given in Fig. 3 (Top) for three different nuclear densities and  $\alpha$  of Eq. (11) set to zero. Interpreting the density dependence of the cross section at fixed  $\sqrt{s}$  one has to bear in mind, that a cross section in general is a transition amplitude normalized with respect to the flux of the incoming particles and the number of target particles. So the cross section for  $\Delta^- p \rightarrow nn\eta$  as plotted in Fig. 3 does not contain the probability for a  $\Delta$  meeting a nucleon, which does, of course, also depend on the density.

Keeping this in mind the density dependence of the cross section at fixed  $\sqrt{s}$  is easy to understand. It becomes smaller with increasing  $\rho$ , because the probability for the exchanged pion to react with the medium grows with the density. In the  $\sqrt{s}$ -region where the pion can be on-shell (see Sec. 2.3) the total cross section scales roughly with  $1/\rho$  and diverges for vanishing density.

Fig. 3 (Bottom) shows the cross section with and without the exchange of a  $\rho$ -meson. One sees that the process  $\Delta N \rightarrow NN\eta$  is clearly dominated



by the exchange of the pion (The coupling constants used were given in Eq. (7)). A more recent analysis [13] finds a  $\Delta$ - $N$ - $\rho$ -coupling which is about a factor of two below the one given in Eq. (7), so that the contribution of the  $\rho$ -exchange is even smaller. The large contribution of the  $\rho$ -exchange found for  $NN \rightarrow NN\eta$  in [6, 7] does not appear here, because the on-shell pion dominates the reaction.

### 3 Comparison to the BUU-Parameterization

The purpose of this work is to provide microscopically justified input for transport theories like the BUU-model to describe the production of  $\eta$ -mesons in heavy ion collisions. In standard BUU-calculations [14] the process  $\Delta N \rightarrow NN\eta$  is implemented in two additive ways:

- 1. Sequential production:** A  $\Delta$ -resonance can decay into a nucleon and a pion, that is treated as a real, on-shell particle. One of the possible reactions for this pion is then  $\pi N \rightarrow N\eta$ .
- 2. Direct production:** One of the reactions allowed for the  $\Delta$  besides the decay is the direct production of an  $\eta$ -meson via  $\Delta N \rightarrow NN\eta$ . The cross section for this process was assumed to be equal to the cross section for  $NN \rightarrow NN\eta$  at the same  $\sqrt{s}$ , corrected for the different spin-isospin degeneracies in the entrance channel.

In the last section it was shown, that the total cross section is governed by the exchange of an in-medium pion with a finite width. Consequently the contribution to the  $\eta$ -production by on- and off-shell pions cannot strictly be separated. Indeed, Salcedo et al. [15] have shown for a similar problem that

in the limit of vanishing density the sequential and the direct production processes give exactly the same result. Thus, a BUU-calculation employing both the sequential and the direct production channel might contain some double counting. This is the point we want to investigate in the following discussions.

In order to do so we consider a single  $\Delta$ -resonance of given energy moving in homogeneous matter with density  $\rho$  and calculate the  $\eta$  production rate by solving appropriate rate equations. For simplicity we take one definite isospin channel, namely a  $\Delta^-$  moving within a medium of protons. In this channel the additional cross sections we will need below are experimentally well known. Also for simplicity we first set  $\tilde{\Gamma}_\pi(\rho)$  of Eq. (10) equal to zero, thus neglecting many-body reactions of the pion; these effects will be discussed separately at the end of this section.

The rate equations have to contain the decay widths and reaction rates of all possible processes. These are for the

**$\Delta$  channels:**

**$\Delta$ -decay:** This enters into the rate equations via the decay width  $\Gamma_\Delta$ .

In our scenario there is no medium modification of this width due to Pauli blocking, because a  $\Delta^-$  can only decay into a  $\pi^-$  and a neutron, for which there is no Pauli blocking in a medium of protons.

**$\Delta$ -absorption:** Given the cross section for  $\Delta N \rightarrow NN$  [14] the reaction rate for this reads:

$$\Gamma_{\Delta p \rightarrow nn} = v_\Delta \sigma_{\Delta p \rightarrow nn} \rho \quad (12)$$

where  $v_\Delta$  is the velocity of the  $\Delta$  and  $\rho$  is the density of the

protons.

**Direct  $\eta$ -production:** The reaction rate for this is given by:

$$\Gamma_{\Delta p \rightarrow nn\eta} = v_{\Delta} \sigma_{\Delta p \rightarrow nn\eta} \rho . \quad (13)$$

So far, no sequential production is included. To account for it we have to consider the reactions that the pion produced by the decay of the  $\Delta$  can undergo:

**Secondary  $\pi$  interactions:**

**Reaction with the medium:** Using the total pion-nucleon cross section, which appeared already in Eq. (10), the reaction rate for this is:

$$\Gamma_{\pi p} = v_{\pi} \sigma_{\pi p} \rho \quad (14)$$

As has been said before, being the total cross section  $\sigma_{\pi p}$  contains elastic and inelastic processes.

**$\eta$ -production:** Our calculation for the cross section for  $\pi p \rightarrow n\eta$  are shown in Fig. 2 together with experimental data. With that cross section the reaction rate is:

$$\Gamma_{\pi p \rightarrow n\eta} = v_{\pi} \sigma_{\pi p \rightarrow n\eta} \rho \quad (15)$$

Combining all these channels we arrive at the following rate equations:

$$\begin{aligned} \frac{d}{dt} N_{\Delta}(t) &= (-\Gamma_{\Delta p \rightarrow nn} - \Gamma_{\Delta} - \Gamma_{\Delta p \rightarrow nn\eta}) N_{\Delta}(t) \\ \frac{d}{dt} N_{\pi}(t) &= \Gamma_{\Delta} N_{\Delta}(t) - \Gamma_{\pi p} N_{\pi}(t) \\ \frac{d}{dt} N_{\eta}(t) &= \Gamma_{\Delta p \rightarrow nn\eta} N_{\Delta}(t) + \Gamma_{\pi p \rightarrow n\eta} N_{\pi}(t) . \end{aligned} \quad (16)$$

These equations constitute a first collision model; as such they do not contain any refeeding of the  $\Delta$  or of the  $\pi$ . This is not only sufficient for our purpose of comparing the BUU-prescription with our microscopic calculation, but is even a cleaner test because it does not sum over complicated collision histories with their inherent averaging over many processes and cross sections.

The first of Eqs. (16) contains some double counting, because on-shell pions appear both in  $\Gamma_\Delta$  and  $\Gamma_{\Delta p \rightarrow nn\eta}$ . However, for normal nuclear density it is  $\Gamma_{\Delta p \rightarrow nn\eta} \approx 0.01 \Gamma_\Delta$ , so that this double counting has negligible consequences.

Because of the absence of any refeeding terms in the  $\Delta$  and  $\pi$  channels Eqs. (16) can easily be solved. If one uses the initial conditions  $N_\Delta(0) = 1$ ;  $N_\pi(0) = N_\eta(0) = 0$  and takes the limit  $P_\eta = \lim_{t \rightarrow \infty} N_\eta(t)$ , then  $P_\eta$  is the probability for the production of an  $\eta$ -meson in the first reaction of either the  $\Delta$  or the pion produced in the decay of that  $\Delta$  with a proton of the medium.

If the density dependent cross section calculated above is used in Eq. (13) for  $\Gamma_{\Delta p \rightarrow nn\eta}$ , the width  $\Gamma_{\pi p \rightarrow n\eta}$  has to be set equal to zero, because then the cross section  $\sigma_{\Delta p \rightarrow nn\eta}$  already contains all kinematically possible invariant masses of the intermediate pion. The results of this calculation are shown in Fig. 4 (upper curves). The density dependence of  $P_\eta$  is weak because the approximate  $1/\rho$ -dependence of the cross section is multiplied with the  $\rho$ -dependence of the collision rate (Eq. 13).

Also shown in Fig. 4 is the result for the sequential process, obtained by setting  $\sigma_{\Delta p \rightarrow nn\eta}$  to zero in the rate equations given above (lower curves). For  $\rho = \rho_0$  the sequential  $\eta$ -production probability is about 30 % smaller

than the direct production cross section given by the upper curves. For decreasing density, however, the upper and the lower curves converge and for  $\rho \rightarrow 0$  they coincide, in agreement with the theoretical results of Salcedo et al [15]. The physical reason for this is that for  $\rho \rightarrow 0$  the pion has to travel an arbitrarily long distance before reacting with a nucleon. This can only happen, if the pion is strictly on shell, so that the sequential description becomes exact, and the upper and lower curves in Fig. 4 have to coincide. The difference between the two sets of curves thus reflects an important in-medium effect.

It can also be seen from Fig. 4, that at finite density the direct  $\eta$ -production and the sequential process have different thresholds. This is due to the fact that the sequential threshold lies above the absolute energy threshold for  $\eta$  production in the  $\Delta N$  channel because the requirement of an on-shell pion constitutes an additional constraint on the reaction dynamics (see Sec. 2.3). Only for  $\rho = 0$  both thresholds agree, in agreement with the theoretical considerations of Salcedo et al.

The Fermi momentum of the protons is not taken into account in Fig. 4. Including this leads to a smearing of all curves over a certain energy range, which blurs the differences shown in Fig. 4.

In order to check the validity of the parameterization of the direct production cross section and the inclusion of both direct and sequential production channels in standard BUU-calculations we now compare our results with calculations that treat the possible reaction channels like the BUU-model. In the context of our scenario this means that we have to include in the rate equations both the sequential production as in Fig. 4 and the direct production process, but now with the density-independent parameterization

given in [14] for  $\sigma_{\Delta p \rightarrow nn\eta}$ . This does not change the result in the limit of  $\rho \rightarrow 0$  because in this case  $\Gamma_{\Delta p \rightarrow nn\eta}$  vanishes while  $\Gamma_{\Delta}$  remains constant (first of Eqs. 16). The two contributions together with the resulting total production probability are shown in Fig. 5.

Fig. 6 (Top) shows a comparison of the results of the BUU-simulation including both the direct BUU-type production and the sequential channel (i.e. of the results of Fig. 5) with the results of the calculations employing our density dependent cross section for the direct channel only. The two curves are remarkably similar although there is some difference in their energy dependence. This difference is mainly due to a somewhat different energy dependence of the calculated cross section for  $\Delta N \rightarrow NN\eta$  and its BUU-parameterization. Taking the Fermi motion into account diminishes this difference significantly (Fig. 6 (Bottom)). The agreement between the two prescriptions at other densities than  $\rho_0$  is similar.

So far, all the calculations have neglected the contribution of many-body effects on the pion selfenergy. Fig. 7 now shows results for two different values of  $\alpha(\rho_0)$  of Eq. (11), entering via the pion selfenergy and Eq. (14), respectively. In both cases the agreement between the BUU prescription and the calculation with our calculated cross section is still very reasonable for low to intermediate kinetic energies of the  $\Delta$  ( $T_{\Delta} < 1$  GeV). This agreement for different values of  $\alpha$  is due to the fact that the replacement (11) affects the results of both models in an analogous way by causing a higher reaction probability of the pion. Only at higher energies we obtain a stronger dependence of  $P_{\eta}$  on  $\alpha(\rho_0)$  than in the BUU-case. This is simply due to the fact that in the BUU-case the cross section for the direct process is taken to be density-independent, so that in this case only the sequential

production depends on  $\alpha$ .

## 4 Conclusion

We have calculated the cross section for  $\Delta N \rightarrow NN\eta$  in a microscopical model using empirical interaction vertices. Because of the special kinematics of this reaction, the exchanged pion can be on-shell so that a straightforward evaluation of the corresponding Feynman graphs leads to divergent results. By including in-medium effects, however, we have obtained a finite, density dependent result. This result contains all kinematically possible situations, including the point, where the invariant mass of the exchanged pion is equal to its free mass.

We have then used this cross section to check the ad-hoc treatment of the  $\Delta N$  channel for particle production in transport theories like the BUU-model. This is essential, because at energies far below threshold  $\eta$ -mesons are created mainly via the resonance channel.

The BUU-prescription allows both the direct and the sequential process. The sequential production involves a pion which is propagated as an on-shell particle, while the direct process is included on an ad-hoc basis with a guessed cross section to account for the  $\eta$ -production via off-shell pions. In order to compare our ‘exact’ calculation with this BUU-recipe we have set up a simple scenario in which the probability for the initial production of an  $\eta$ -meson by a  $\Delta$  of given energy was calculated for both cases by solving rate equations.

As a result we have found, that by allowing sequential production alone one obtains an  $\eta$ -yield, which was clearly below the one obtained with the

cross section calculated in this work (Fig. 4). Only if we included sequential and direct production at the same time, using the cross sections as given in [14], the correct  $\eta$ -production probability was reproduced quite well (Fig. 6, Top). The different energy dependence still visible there vanished nearly completely when the Fermi distribution of the medium was taken into account (Fig. 6, Bottom). We thus conclude, that there is no double counting in the BUU-treatment and that the BUU-recipe for the  $\Delta N \rightarrow NN\eta$  cross section works surprisingly well. This result puts the enhancement of far-subthreshold particle production obtained in BUU-calculations on a firmer basis.

## References

- [1] V. Metag, Prog. Part. Nucl. Phys, **30**, (1993) 75
- [2] W. Ehehalt et al., Phys. Rev. **C47** (1993) 47.
- [3] U. Mosel, Ann. Rev. Part. Sci. **41** (1991) 29
- [4] W. Cassing, Phys. Scr. **48** (1993) 194
- [5] T. Vetter et al., Phys. Lett. **B263** (1991) 153
- [6] J. M. Laget et al., Phys. Lett. **B257** (1991) 254
- [7] J.-F. Germond and C. Wilkin, J. Phys. **G15** (1989) 437
- [8] R. S. Bhalearo et al., Phys. Rev. Lett. **54** (1985) 865
- [9] Particle Data Group, *Review of Particle Properties*, Phys. Rev. **D50** Part 3-I.



- [10] Landolt-Börnstein *Total Crosssections for Reactions of High-Energy Particles*, Band I/12a, Berlin 1973.
- [11] T. Ericson and W. Weise, *Pions and Nuclei*, Clarendon, Oxford, 1988.
- [12] L. L. Salcedo et al., Nucl. Phys. **A 484** (1988) 557
- [13] M. SchΞfer et al., Nucl. Phys. **A 575** (1994) 429.
- [14] G. Wolf et al., Nucl. Phys. **A545** (1992) 139.
- [15] L. L. Salcedo et al., Phys. Lett. **B208** (1988) 339

Figure 1: Top: Diagrams dominating the process  $\Delta N \rightarrow NN\eta$ . Bottom: Diagrams contributing to the process  $\pi N \rightarrow N\eta$ .

Figure 2: Experimental data for the cross section for  $\pi^- p \rightarrow n\eta$  together with our calculations like described in the text. The data were taken from [10].

Figure 3: Total cross section for  $\Delta^- p \rightarrow nn\eta$ . Top: Assuming three different nuclear densities. Bottom: With and without the  $\rho$ -exchange ( $\rho = \rho_0$ ).

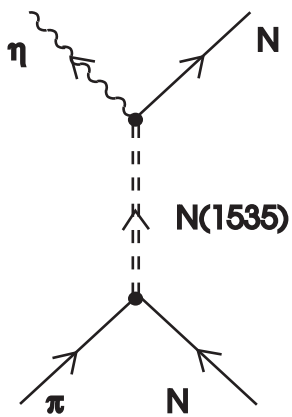
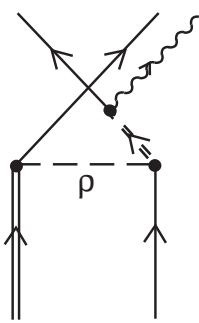
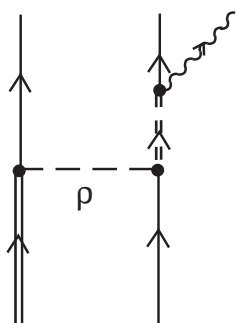
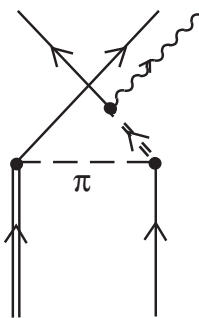
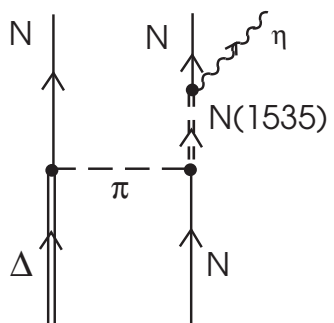
Figure 4:  $\eta$ -production probability for different densities using only the direct process with the density dependent cross section (upper curves) and using only the sequential production (lower curves) without Fermi motion.

Figure 5: Total  $\eta$ -production probability in a BUU scenario (solid curve). The lowest (dotted) curve gives the direct production probability obtained using the BUU-parameterization. The dashed curve shows the sequential contribution (same as in Fig. 4).

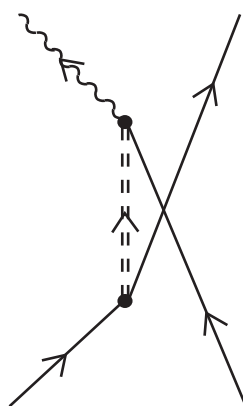
Figure 6: Top:  $\eta$ -production probability using only the direct process with the density dependent cross section calculated in this paper and using the sum of the sequential and the direct process in the BUU-parameterization (for  $\rho = \rho_0$ ). Top: Without Fermi motion. Bottom: With Fermi motion.

Figure 7:  $\eta$ -production probability for two different values of  $\alpha(\rho_0)$  of Eq. (11) (with Fermi motion,  $\rho = \rho_0$ )

.

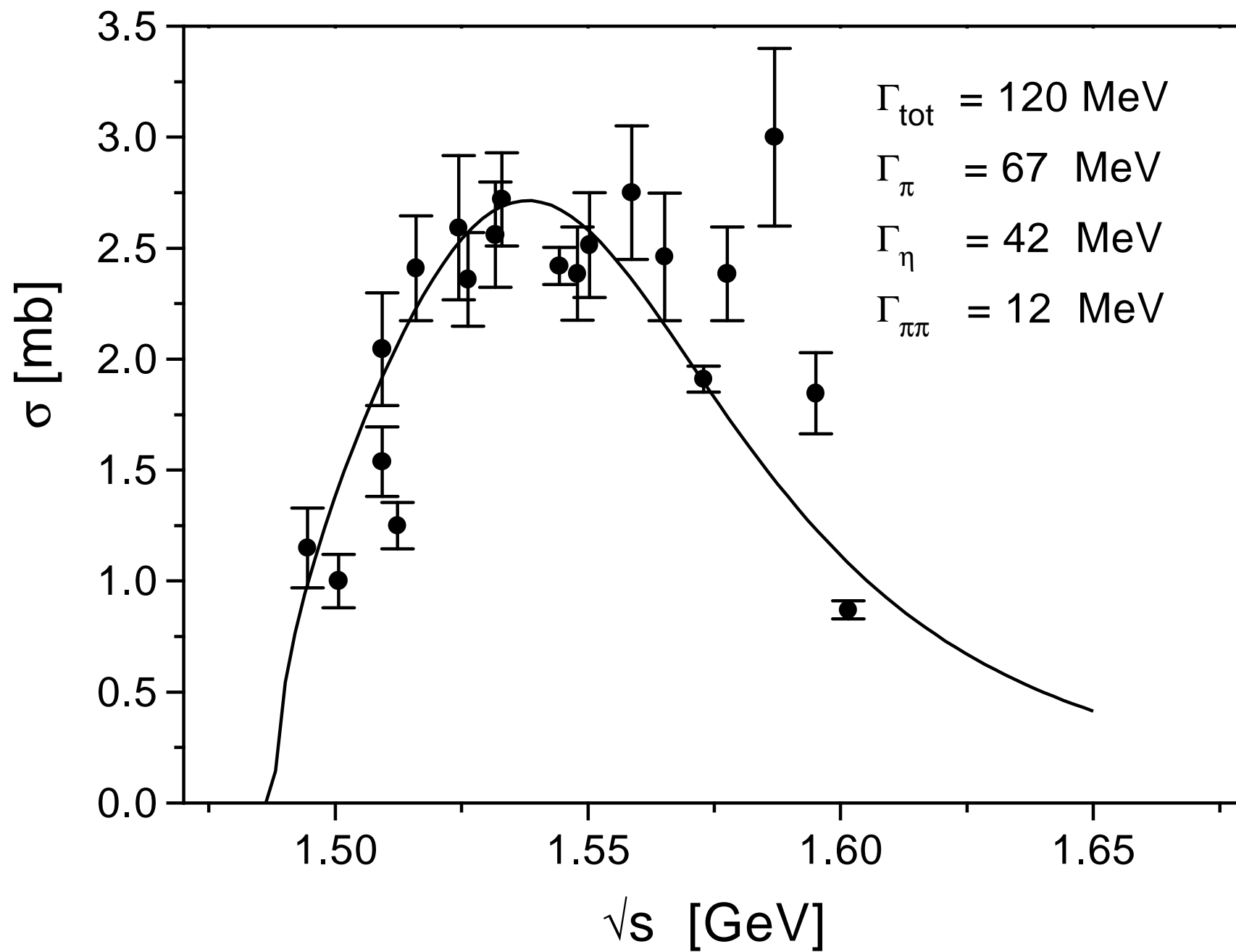


+



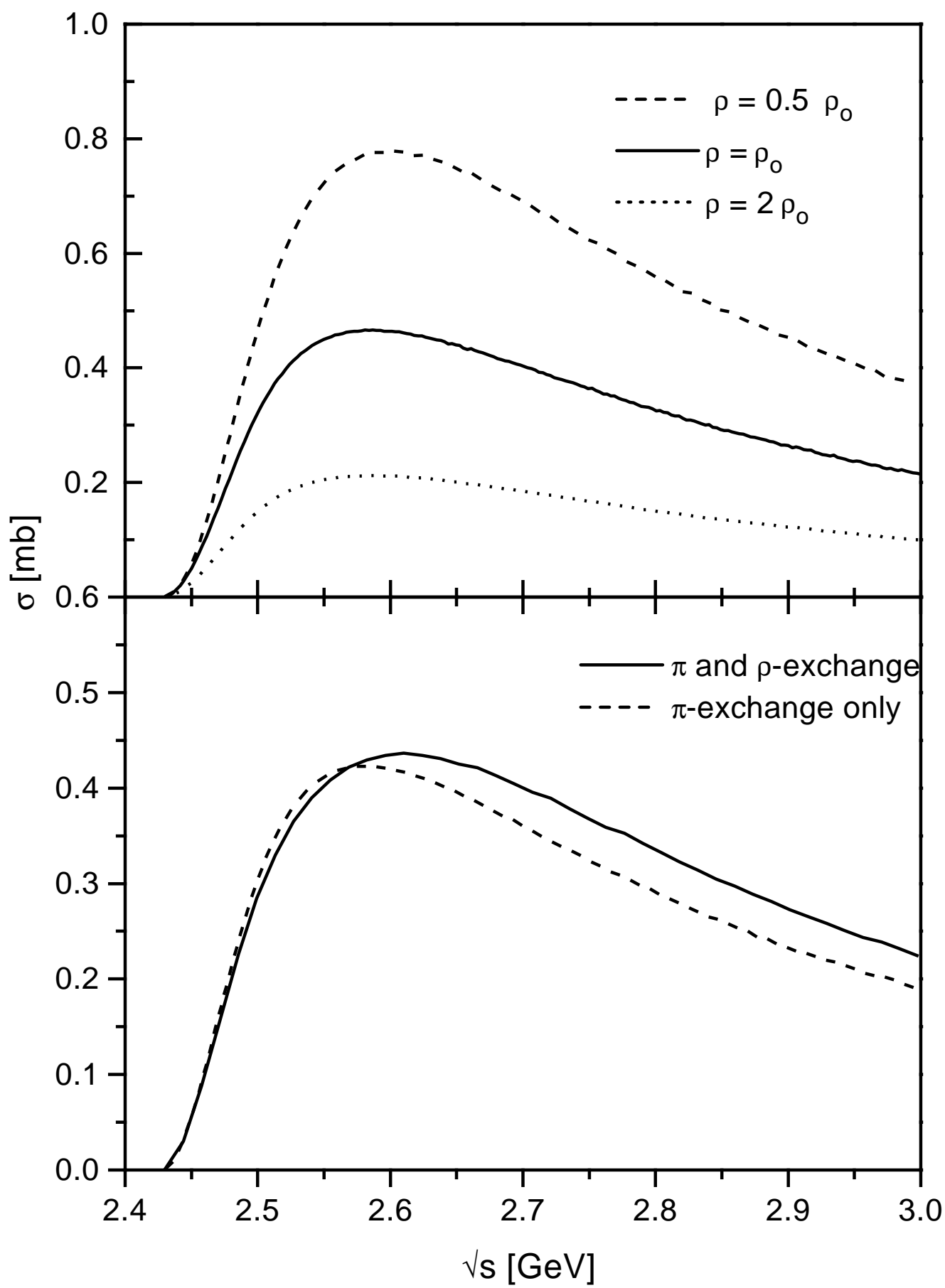
This figure "fig1-1.png" is available in "png" format from:

<http://arXiv.org/ps/nucl-th/9407031v2>



This figure "fig1-2.png" is available in "png" format from:

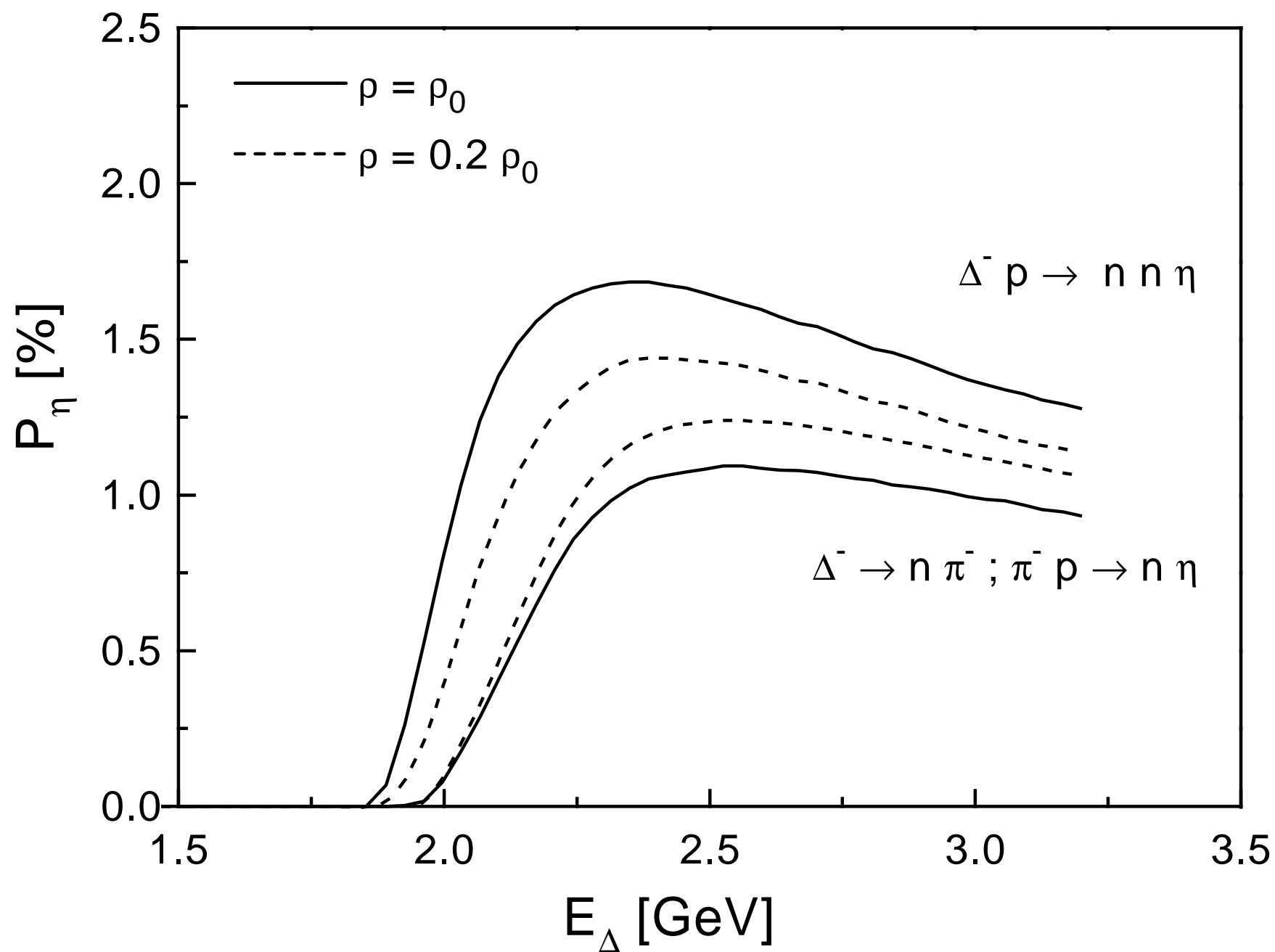
<http://arXiv.org/ps/nucl-th/9407031v2>



This figure "fig1-3.png" is available in "png" format from:

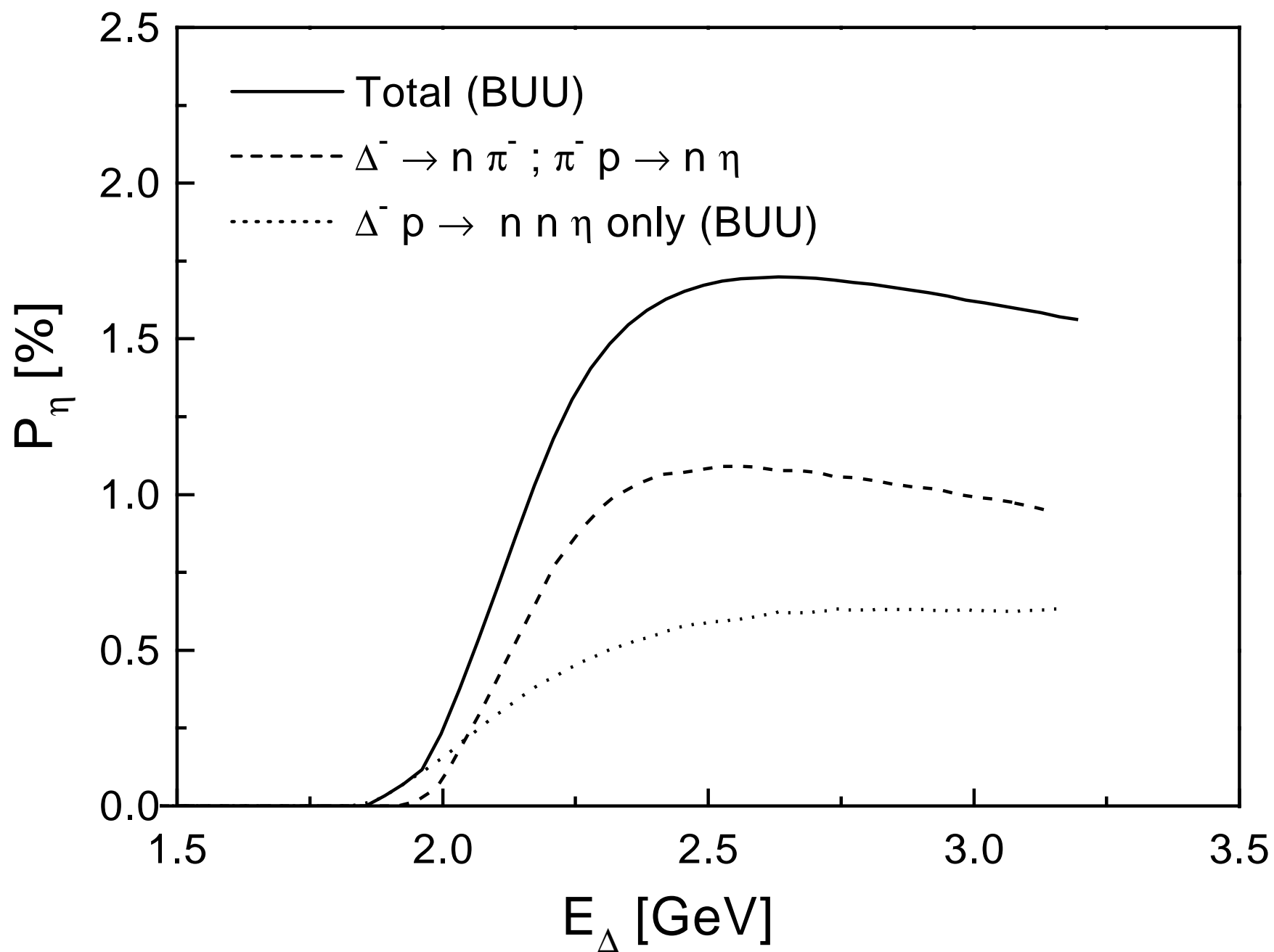
<http://arXiv.org/ps/nucl-th/9407031v2>





This figure "fig1-4.png" is available in "png" format from:

<http://arXiv.org/ps/nucl-th/9407031v2>



This figure "fig1-5.png" is available in "png" format from:

<http://arXiv.org/ps/nucl-th/9407031v2>

